

# Magneto-mechanical modeling of a tubular permanent magnet linear generator for wave energy conversion using T-Omega formulation

*Badanie projektu rurowego liniowego generatora z trwałymi magnesami do przekształcania energii fal przy zastosowaniu formuły T-Omega*

**Abstract.** This article explores the design and simulation of a Tubular Permanent Magnet Linear Generator (TPMLG) for wave energy conversion using the Finite Element Method (FEM). The proposed approach employs the T-Omega formulation to significantly reduce computational time compared to conventional FEM formulations while maintaining simulation accuracy. A coupled magneto-mechanical model captures essential electromagnetic-structural interactions critical for TPMLG performance. Experimental data validate the accuracy and reliability of the T-Omega formulation in modeling TPMLG behavior. The proposed approach enables rapid design optimization of TPMLGs, accelerating the practical implementation of wave energy conversion systems.

**Streszczenie.** Niniejszy artykuł bada projektowanie i symulację rurowego liniowego generatora z magnesami trwałymi (LGMT) do konwersji energii fal przy użyciu metody elementów skończonych. Zaproponowane podejście wykorzystuje formułę T-Omega, aby znacząco zmniejszyć czas obliczeniowy w porównaniu z konwencjonalnymi technikami, przy zachowaniu dokładności symulacji. Sprzężony model magneto-mechaniczny uwzględnia kluczowe oddziaływania elektromagnetyczno-strukturalne istotne dla wydajności generatora. Dane eksperymentalne potwierdzają dokładność i wiarygodność formuły T-Omega w modelowaniu zachowania LGMT. Zaproponowane podejście umożliwia szybką optymalizację projektową generatora, przyspieszając praktyczne wdrożenie systemów konwersji energii fal.

**Keywords:** Finite element method, T-Omega formulation, tubular linear generator, wave energy conversion

**Słowa kluczowe:** Metoda elementów skończonych, formuła T-Omega, liniowy generator rurowy, konwersja energii falowej

## Introduction

The increasing demand for renewable energy sources has spurred the advancement of a variety of wave energy conversion systems including point absorbers, oscillating water columns, overtopping devices, and linear generators. Point absorbers use a buoyant device that oscillates with the waves and drives a power take-off system, while oscillating water columns utilize the movement of air inside a column to drive a turbine. Overtopping devices capture the wave's energy by allowing it to flow into a reservoir, which then drives a hydro turbine. Each of the systems mentioned above has limitations, such as the requirement of a large space or complex control procedure. Linear generators, on the other hand, offer a compact and efficient solution that can be directly coupled with the wave energy conversion system, eliminating the need for complex power take-off systems [1, 2].

Linear generators have gained attention as a promising solution for wave energy conversion systems due to their high efficiency and direct drive capability. Especially, Permanent Magnet Linear Generators (PMLGs) have gained popularity due to their high power density [3]. This high power density is crucial for offshore applications where space is limited. Additionally, they offer a high magnetic flux density, which enhances their power output and improves their overall efficiency. The stationary coils and moving magnets of PMLGs eliminate the need for a ferromagnetic core or additional power sources, resulting in a more compact and lightweight generator design [4].

The Finite Element Method (FEM) is a powerful technique that is highly effective in the design and simulation of PMLGs. FEM is a computational technique used to analyze and optimize the performance of complex systems, such as the electromagnetic and mechanical behavior of PMLGs. It allows designers to model and simulate the behavior of PMLGs under different operating conditions, and to identify potential issues and areas for improvement in the generator's design [5].

The following studies have extensively employed FEM to optimize the design and performance of PMLGs for wave energy conversion. In [6], a novel TPMLG is proposed for direct-drive wave energy conversion. By integrating two TLPMLGs into a single device, the design enhances power output from a single translator stroke. The study presents design details and validates the generator's high performance, specifically its output voltage, power, and force densities, through 2D and 3D finite element analysis. In [7], a novel Linear Permanent Magnet Vernier Machine (LPMVM) with consequent-pole and halbach Permanent Magnet arrays is developed. The LPMVM shows a substantial increase in the thrust density and the no load back Electromotive Force (EMF) compared to traditional LPMVMs. Various analysis methods, including Analytical Method, Equivalent Magnetic Circuit Method and FEM, are examined, with FEM ultimately chosen for electromagnetic analysis. In [8], a novel design of a speed-amplified linear generator for the power take-off unit of an ocean wave energy converter is presented. The design integrates innovative features such as semi-closed stator iron cores, four-phase coil shifting, and a fixed pulley wheel mechanism that effectively doubles the translator's relative speed. A 3D FEM model is developed and optimized using sinusoidal wave excitation to enhance output power and reduce cogging force. In [9], a new TPMLG is introduced, featuring armature windings embedded within the slots of modulating segments. This innovative design increases thrust density, reduces cogging force, and enhances overall mechanical efficiency. In [10], a modular TPMLG is proposed, comprising a stationary primary section with concentrated three-phase windings and a moving secondary section equipped with permanent magnets. This customized design allows different lengths to be assembled according to power requirements. FEM was employed to analyze the effect of design factors, such as the size and shape of the magnets and coils, on the generator's efficiency and to optimize the design accordingly.

The use of FEM in engineering design and simulation is a time-consuming process that requires substantial computational resources. The process involves the creation of a complex mathematical model that is then analyzed through iterative computations. While FEM offers a valuable understanding of the behavior and performance of engineering systems, it can be prohibitively time-consuming, particularly for complex systems.

One solution to reducing the time required for FEM simulations is the use of the T-Omega mathematical formulation [11-13]. This formulation is a computationally efficient method for simulating the performance of engineering systems, including electromagnetic devices. The T-Omega formulation uses a simplified mathematical model that reduces the computational cost of simulations while maintaining accuracy. Moreover, the T-Omega formulation offers insights into the behavior and performance of engineering systems that would be difficult to obtain through traditional FEM formulations. As such, the T-Omega formulation offers a promising solution to the time-consuming nature of FEM simulations and has significant potential for optimizing the design and performance of engineering systems in a broad range of applications.

This paper investigates the performance of a TPMLG for wave energy conversion using the T-Omega formulation. The proposed approach employs the electric vector potential ( $T$ ) and the magnetic scalar potential ( $\Omega$ ) to significantly reduce computational costs by simplifying the problem to a single degree of freedom in non-conducting regions. The TPMLG is simulated using this formulation, and the results are validated against experimental data to ensure accuracy and reliability. Furthermore, a magneto-mechanical model is incorporated to analyze the coupling between magnetic fields and structural mechanics, providing a comprehensive understanding of the generator's behavior. The proposed approach achieves a computationally efficient yet highly accurate simulation method, offering a more effective and reliable framework for designing and optimizing TPMLGs for wave energy conversion, supporting the advancement of this renewable energy technology.

### The working principle of permanent magnet linear generator

A TPMLG consists of a tubular stator and a moving translator that is driven by the wave motion as illustrated in Fig.1. The stator has a series of axial slots that are evenly spaced around the circumference of the tube. The slots are wound with copper wire to form coils that are connected in series or parallel to achieve the desired output voltage and power. The translator is composed of a permanent magnet array that moves along the length of the stator as the wave passes by. The motion of the magnet array through the coils induces an EMF in the coils, which generates an alternating current (AC) output.

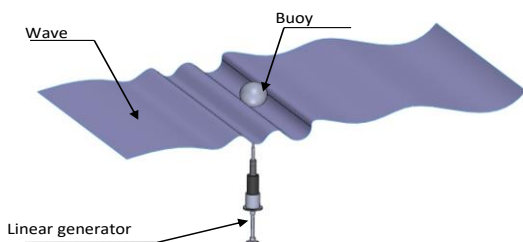


Fig. 1. Schematic representation of sea wave energy conversion systems

### Magneto-mechanical modeling

In the TPMLG, the magneto-mechanical coupling mechanism is a critical factor in determining the overall system performance [16]. The magnetic field produced by the permanent magnets interacts with the movement of the translator, resulting in the induction of eddy currents in the conducting components of the generator. These eddy currents, in turn, create a magnetic field that interacts with the permanent magnets, generating a force that opposes the movement of the translator. This force is known as the magnetic damping force, which limits the maximum power output of the generator [17]. Therefore, a proper design and control of the system is necessary to balance the magnetic damping and the electromagnetic forces, optimizing the energy conversion efficiency of the TPMLG.

### Mechanical Model

The mechanical modeling of a TPMLG involves the consideration of the hydrodynamic forces acting on the float as it moves in the water. The hydrodynamic forces are modeled using fluid dynamics principles, such as the Navier-Stokes equations, to predict the fluid flow around the float [18-20]. The float motion equation is then used to describe the dynamics of the float in response to the hydrodynamic forces. The mechanical modeling of the PMLGs also includes the modeling of the structural components of the generator, such as the stator and rotor, and the interactions between the mechanical and magnetic fields. The goal of mechanical modeling is to optimize the design of the generator for maximum efficiency and performance. By accurately modeling the magneto-mechanical coupling, it is possible to predict the behavior of the generator under various operating conditions and to identify potential design improvements.

### Hydrodynamic Modeling

From the point of view of fluid mechanics, the physics of the flow associated with the swell is incompressible and irrotational [21], that is to say:

$$\begin{aligned} (1) \quad & \text{div} \vec{V} = 0 \\ (2) \quad & \text{rot} \vec{V} = 0 \end{aligned}$$

With:  $\vec{V}$  – is the fluid velocity.

The wave is assumed to propagate from left to right in the positive x-direction; thus, the free surface profile is described by:

$$\begin{aligned} (3) \quad & \eta(x,t) = A \cos(kx - \omega t) \\ (4) \quad & \varphi(x,z,t) = \frac{Ag}{\omega} \frac{chk(z+h)}{chkh} \sin(kx - \omega t) \end{aligned}$$

Where  $A$  – represents the wave amplitude, defined as  $A = H/2$ , with  $H$  – being the wave height. The spatial frequency  $2\pi/L$  – corresponds to the wavelength  $L$ , and the temporal frequency  $\omega = 2\pi/T$  – is associated with the wave period  $T$ . The spatial and temporal frequencies are interconnected by the dispersion relation, expressed as:

$$(5) \quad \omega^2 = gk \tanh(kh)$$

Where  $g$  represents the acceleration due to gravity, and  $h$  the water depth. Meanwhile, the overall profile of the irregular wave can be described by:

$$(6) \quad \eta(x,t) = \sum \eta_i \cos(k_i x - \omega_i t - \varphi_i)$$

With:  $\varphi_i$  – is the random phase,  $i$  – represents the wave component identified by its index.

## Float motion equation

The books of [21] and [22] were used as references to explain the behavior of the system. An oscillating buoy type energy converter is subjected to different forces: The force of gravity, the thrust of Archimedes, the excitation forces (related to the indexed and diffracted wave potential), the radiation effect, the forces related to the electromagnetic converter.

To write the equation of motion of the system, the balance of the global forces acting on the float is applied. Using the fundamental principle of dynamics, this is reported in equation (7).

$$(7) \quad m\ddot{z} = p + \Pi + F_r + F_{em} + F_{ex}$$

Where:  $m$  – is the dry mass of the buoy,  $\ddot{z}$  – is the acceleration of the floating buoy,  $p$  – denotes the force of gravity,  $\Pi$  – the buoyancy of Archimedes,  $F_{ex}$  and  $F_r$  – represent respectively the forces of excitation and the effect of radiation, while  $z(t)$  – expresses the center of gravity position of the float.

The excitation force is calculated from the hydrodynamic pressure equation (8), thus presented in equation (9), where  $S$  – represents the surface of the float. The radiation effect  $F_r$  depends on the radiated potential  $\varphi_r$ .

It corresponds to the forces acting on the moving float in calm water. Like the excitation forces, it is calculated from the pressure as expressed in equation (10). The electromagnetic force  $F_{em}$  is calculated in equation (11).

$$(8) \quad p = p_0 - \rho g z - \rho \frac{\partial \varphi}{\partial t} - \frac{1}{2} \rho (grad \varphi)^2$$

$$(9) \quad F_{ex} = -\rho \frac{\partial (\varphi_I + \varphi_D)}{\partial t} ds$$

$$(10) \quad F_r = -\rho \frac{\partial \varphi_r}{\partial t} ds$$

$$(11) \quad F_{em} = B.I(2Nl \sin(\theta) + Gl^2(2 \sin(2\theta)))$$

Where:  $p_0$  – the reference pressure is equal to atmospheric pressure;  $\rho$  – The density of seawater;  $\varphi_D$  – diffracted wave potential;  $\varphi_I$  – Incident wave potential;  $B$  – is the magnetic flux density;  $I$  – is the electric current intensity;  $N$  – is the number of turns in each phase;  $l$  – is the length of the conductor;  $\theta$  – is the phase angle between the electric current and the magnetic flux; and  $G$  – is the electromechanical coupling constant.

The excitation and damping strength of the radiation found using a linear version of Morison's equations [23, 24]. can be written as:

$$(12) \quad F_{ex} = \zeta \dot{\eta} + \lambda \dot{\eta} + K\eta(t)$$

$$(13) \quad F_r = -\zeta \dot{z} - \lambda \dot{z}$$

$$(14) \quad k = -\rho g \pi r^2$$

Where:  $\zeta$  – represents the added mass,  $\lambda$  – is the radiation damping term,  $r$  – the float radius, and  $K$  – the hydrostatic stiffness.

Equation (15) represents the hydrodynamic model; the electromechanical coupling is ensured by the electromagnetic force.

$$(15) \quad \frac{d}{dt} \begin{bmatrix} \dot{z} \\ \ddot{z} \end{bmatrix} = \begin{bmatrix} -\lambda & -k \\ m+\zeta & 0 \end{bmatrix} \begin{bmatrix} \dot{z} \\ \ddot{z} \end{bmatrix} - \begin{bmatrix} 1 \\ m+\zeta \\ 0 \end{bmatrix} [F_{em}] + \begin{bmatrix} 1 \\ m+\zeta \\ 0 \end{bmatrix} [F_{ex}]$$

## Electromagnetic Model

The T-Omega formulation is employed in this study to handle the problem of electromagnetic eddy current. This approach leverages the electric vector potential and the magnetic scalar potential to describe the system's physics. By simplifying the model to consider only one degree of freedom, rather than three, in all non-conducting regions, it significantly lowers computational costs. The numerical model is based on a 3D FEM using tetrahedral elements [25–27]. To simplify the analysis, displacement currents are neglected, assuming the dominance of conduction currents  $J$ , a typical assumption for eddy current problems. This simplification, applied to Ampere's law, ensures that the current density has zero divergence, thereby enforcing closed loops for both induced and source currents.

The fundamental relationship between magnetic and electric fields is defined by a subset of Maxwell's equations as follows:

$$(16) \quad \overrightarrow{rot} \vec{H} = \vec{J}$$

$$(17) \quad \overrightarrow{rot} \vec{E} = -\frac{\partial \vec{B}}{\partial t}$$

$$(18) \quad \overrightarrow{div} \vec{B} = 0$$

The interdependence of the field vectors is further defined by the material's constitutive relationship.

$$(19) \quad \vec{B} = \mu \vec{H}$$

$$(20) \quad \vec{J} = \sigma \vec{E}$$

The interdependence between the electric and magnetic fields is further defined by the material's constitutive relationship, wherein the magnetic permeability  $\mu$  and electrical conductivity  $\sigma$  of the material serve as governing parameters. These parameters may vary in space and are also field-dependent.

The continuity condition for the current density ensures that the total current flowing into a volume is equal to the total current flowing out of it. This is expressed mathematically as the divergence of the current density being equal to zero. In other words, the induced and source currents must form closed loops, which are enforced by neglecting the displacement current in Ampere's law.

$$(21) \quad \overrightarrow{div} \vec{J} = 0$$

Starting from equation (21), the current density is expressed in terms of the electric vector potential, as shown below:

$$(22) \quad \vec{J} = \overrightarrow{rot} \vec{T}$$

It can be observed from equations (16) and (22) that  $\vec{T}$  and  $\vec{H}$  have the same units but differ by the gradient of a scalar.

$$(23) \quad \vec{H} = \vec{T} - \overrightarrow{grad} \Omega$$

Where  $\Omega$  – is a magnetic scalar potential.

From equations (17), (18), and (20), we can derive: In eddy current region

$$(24) \quad \overrightarrow{rot} \left( \frac{1}{\sigma} \overrightarrow{rot} \vec{T} \right) + j\omega \mu (\vec{T} - \overrightarrow{grad} \Omega) = 0$$

And from (18) we obtain: In eddy current region

$$(25) \quad \overrightarrow{div} (\mu (\vec{T} - \overrightarrow{grad} \Omega)) = 0$$

The scalar potential can be used to determine the magnetic field in regions where there is no current.

$$(26) \quad \vec{H} = -\overrightarrow{grad} \Omega$$

Thus from (21), the following is obtained in current-free regions:

$$(27) \quad -\overrightarrow{div} \mu (\overrightarrow{grad} \Omega) = 0$$

The divergence of  $\vec{T}$  – is remains unspecified, leaving both  $\vec{T}$  and  $\Omega$  undefined.

To resolve this ambiguity, defining the divergence of  $\vec{T}$ , along with its curl, is known as selecting a gauge. One of the most commonly used gauge conditions in electromagnetics is the Coulomb gauge, which is defined as:

$$(28) \quad \text{div} \vec{T} = 0$$

This Coulomb gauge condition enables the addition of a term  $\text{div}(\frac{1}{\sigma} \text{div} \vec{T})$ , to the left-hand side of equation (24)

The general equation is given:

$$(29) \quad \text{rot}(\frac{1}{\sigma} \text{rot} \vec{T}) - \text{div}(\frac{1}{\sigma} \text{div} \vec{T}) + \mu \frac{\partial}{\partial t} (\vec{T} - \text{grad} \Omega) = 0$$

$$(30) \quad \vec{H} = -\text{grad} \Omega$$

Within the region comprising permanent magnets:

$$(31) \quad \vec{H} = \vec{H}_c + (\vec{T} - \text{grad} \Omega)$$

With:  $H_c$  – coercive field.

### Electrical circuit model

The electromagnetic generator's equivalent electrical circuit is depicted in Figure. 2, where  $R_{coil}$  and  $L_{coil}$  – correspond to the resistance and inductance of the generator's coil respectively. Additionally,  $R_{load}$  – denotes the external resistance, which serves to characterize the energy regeneration process [29].

The relationship between the circuit current and the induced EMF,  $e$ , is governed by the electrical load connected to the generator, as formulated in the circuit equation (32):

$$(32) \quad E = (R_{coil} + R_{load})i + L_{coil} \frac{di}{dt}$$

The EMF and current are directly proportional to the relative velocity, giving the linear tubular generator inherent self-sensing capabilities.

With the coil inductance neglected, the maximum power loss occurs when the regenerative energy is zero, i.e., when  $R_{load} = 0$  and the stator coils are short-circuited. Conversely, maximum power regeneration is achieved when the external resistance equals the internal resistance, resulting in the highest electromagnetic damping force. The power can be expressed as follows:

$$(33) \quad P = \frac{E^2}{R_{coil} + R_{load}}$$

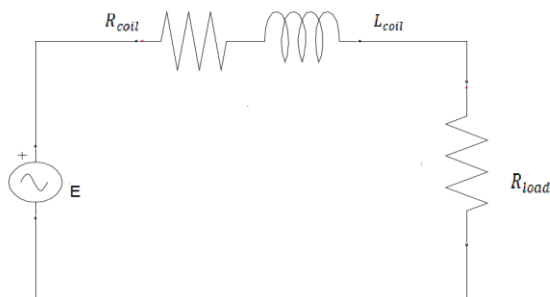


Fig. 2 Equivalent electrical circuit of a wave energy converter system

### Geometric design of a Tubular Permanent Magnet Linear Generator

Figure 3 illustrates the configuration of the TPMLG utilized in the wave energy converter. The setup comprises a stator featuring a three-phase coreless winding, and a mover equipped with axially magnetized NdFeB permanent magnets and a steel pole. This arrangement establishes a magnetic flux path through the iron poles.

The use of axially magnetized NdFeB permanent magnets and iron poles in the magnet topologies facilitates a cost-effective production process. This is due to the ease of magnetization for axially magnetized PMs. Further details regarding dimensions and characteristics can be found in Table 1.

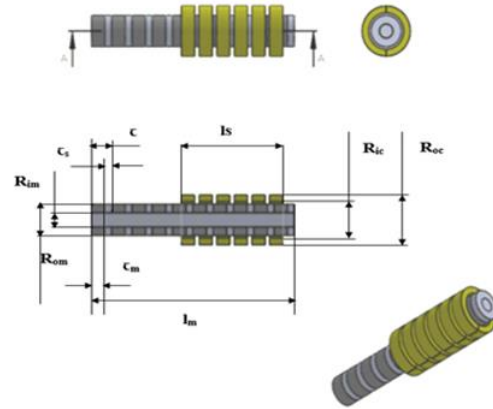


Fig. 3 Geometrical form of a TPMLG

Table 1. Characteristics and dimensions of the employed TPMLG [28]

Components	Symbol	Value
Phases Number	m	3 phases
Pole pitch	c	15 mm
Permanent Magnet width	cm	10 mm
Steel pole width	cs	5 mm
Inner radius of permanent magnet	Rim	10 mm
Outer radius of permanent magnet	Rom	22.5 mm
Air-gap length	δ	3.3 mm
Radius of inner coil	Ric	25.8 mm
Radius of outer coil	Roc	33.4 mm
Mover length	lm	180 mm
Stator length	ls	390 mm
Number of turns per slot	nc	320 turns

### Results and Discussion

The natural heave frequency of the power buoy is deliberately tuned to align with the peak frequency of the wave energy, maximizing the efficiency of energy conversion. This floating wave-energy converter's power generation is directly influenced by the design characteristics of the TPMLG and its associated power take-off system.

The power input, mover stroke, and maximum speed were determined through the analysis of a scaled-down model of the power buoy. This 1/10-scale model was tested in a wave basin, and the results from this analysis were used for the current study.

Figure 4 illustrates the displacement of the power buoy under irregular wave conditions, with a maximum recorded displacement of 0.087 m. Additionally, the simulation results show the time evolution of the piston's speed in Figure 5 and its acceleration in Figure 6, alongside the behavior of the wave.



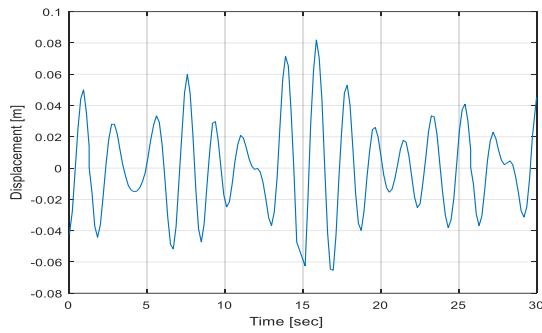


Fig. 4 Displacements of the floating buoy

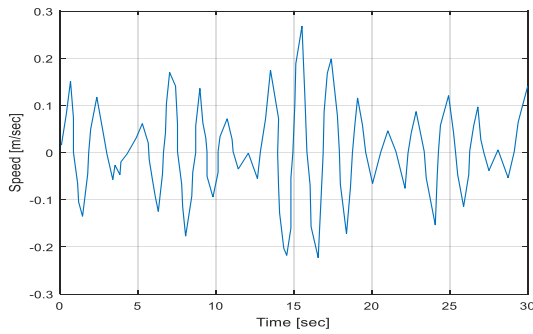


Fig. 5 Speed of the floating buoy

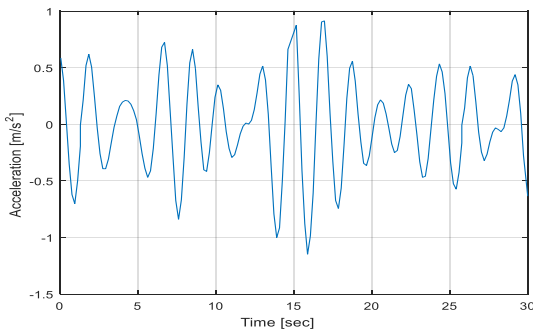


Fig. 6 Acceleration of the floating buoy

Figures 7 and 8 display the variation in magnetic flux density resulting from magnetic excitation, as well as the intensity of the magnetic fields within the TPLMG.

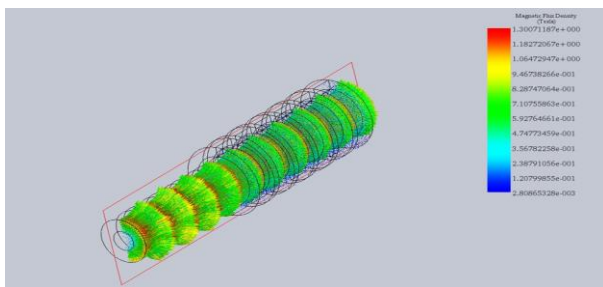


Fig. 7 Distribution of the magnetic flux density

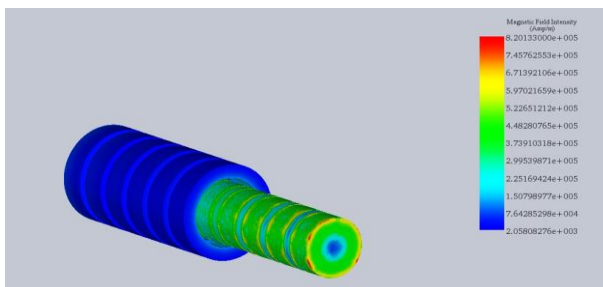


Fig. 8 Intensity of the magnetic fields

Figures 9, 10, and 11 depict the time-varying induced EMF across the three phases of the TPMLG. As predicted by Faraday's law of electromagnetic induction, the induced EMF exhibits a direct proportional relationship with the velocity of the generator. After performing calculations, the total magnitude of the induced EMF is determined to be 1,403 V.

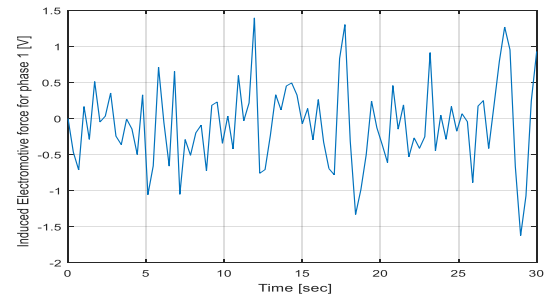


Fig. 9 Induced Electromotive force for phase 1

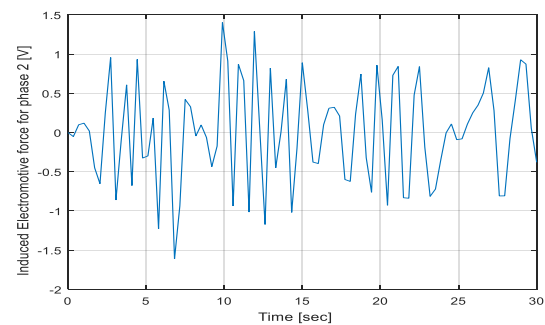


Fig. 10 Induced Electromotive force for phase 2

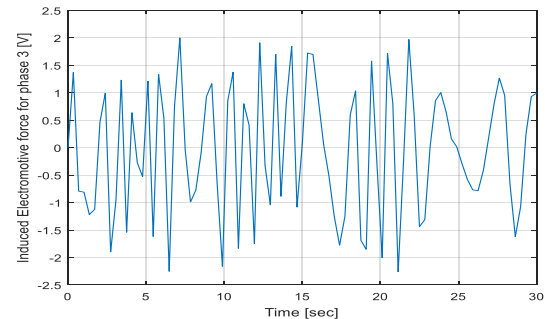


Fig. 11 Induced Electromotive force for phase 3

The comparison of output power between the EMF simulation and the experimental results under irregular wave conditions is illustrated in Figure 12. The attained maximum output power is nearly 3 watts, which fulfills the design requirements. The experimental results demonstrate a strong correspondence with the predictions obtained from the numerical solutions.

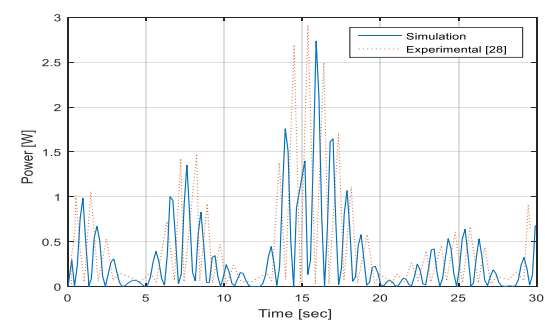


Fig. 12 Electrical output power in linear generator

## Conclusion

This study demonstrates the effectiveness of the T- $\Omega$  formulation for designing and analyzing TPMLGs. The adopted approach provides dual advantages: significantly lower computational costs than conventional finite element formulations while delivering high accuracy, as confirmed by excellent agreement between simulations and experimental data. These results establish the T- $\Omega$  formulation as a reliable and efficient tool for developing optimized TPMLGs for wave energy conversion applications.

**Authors:** Phd student (Corresponding author), Bachir Ouartal, Tizi-Ouzou University, 15000, Algeria, LATAGE Laboratory, E-mail: bachir.ouartel@ummto.dz, Dr. Meziane Hamel, Boumerdès University 35000, Algeria, Laboratory of Energy and Mechanical Engineering (LEMI), E-mail: m.hamel@univ-boumerdes.dz, Prof. Mustapha Zaouia, Tizi-Ouzou University, 15000, Algeria, LATAGE Laboratory, E-mail: mustapha.zaouia@ummto.dz, Dr. Ahmed Nait Ouslimane, Tizi-Ouzou University, 15000, Algeria, Electrical Engineering Dept., E-mail: ahmed.nait\_ouslimane@ummto.dz, Dr. Riad Moualek, Tizi-Ouzou University, 15000, Algeria, LATAGE Laboratory, E-mail: riad.moualek@ummto.dz, Dr. Ratiba Fellag, Advanced Technology Development Center, 16000, Algeria, Robotics and Industrial Automation laboratory, E-mail: rfellag@cdta.dz,

## REFERENCES

- Gayathri R., Jen-Yi C., Chia-Cheng T., & Tai-Wen H., Wave Energy Conversion through Oscillating Water Columns: A Review, *Journal of Marine Science and Engineering*, 12 (2024), 1-22.
- Hongyue C., Naisheng L., & Xianyang L., Wave Energy Linear Generator System Including a Newly Designed Wave Roller Mechanical Interface, *actuators MDPI*, 14 (2025), 1-12.
- Minshuo C., Lei H., Yuan L., Gaojun M., & Tao X., A Low Thrust Ripple Flux-Reversal Transverse Flux Permanent Magnet Linear Generator Used in Direct Drive Wave Energy Converter, *IEEE Transactions on Magnetics*, 60 (2024).
- Domenico C., Vincenzo F., Andrea G., Rosario M., Claudio N., Francesco R., & Marco T., An Experimental Comparison between an Ironless and a Traditional Permanent Magnet Linear Generator for Wave Energy Conversion, *Energies MDPI*, 15 (2022), 1-21.
- Shuheng Q., Wei Z., Chi Z., Jonathan S. & Haifeng W., A Novel Structure of Tubular Staggered Transverse-Flux Permanent-Magnet Linear Generator for Wave Energy Conversion, *IEEE Transactions on Energy Conversion*, 37 (2022), 24-35.
- Neel S., Sashidhar S. & Bidyadhar S., A Novel Dual Magnetically Geared Halbach Array based Tubular Linear Permanent Magnet Generator for Wave Energy Conversion, *IEEE Transactions on Magnetics* (2025), 1-1.
- Chen H., Zhan Y., Wang H. & Nie R., A Tubular Permanent Magnet Linear Generator with Novel Structure, *IEEE transactions on plasma science*, 47, (2019), nr 6, 2995-3001.
- Zhenwei Liu., Cameron McGregor., Songlin Ding., & Xu Wang, Study of a three-dimensional model simulation of a speed amplified flux switching linear generator for wave energy conversion and its design optimization in the ocean environment, *Energy*, 284 (2023).
- Ho S. L., Wang Q., Niu S. & Fu W. N., A novel magnetic-geared tubular linear machine with Halbach permanent-magnet arrays for tidal energy conversion, *IEEE Trans. Magn.*, 51, (2015), nr 11, Art. no. 8113604.
- Ziselimovi M., Sprcic G., Brinovar I., Praunseis Z. & Stumberge B. A novel concept of linear oscillatory synchronous generator designed for a stirling engine, *Energy*, 180, (2019), 19-27.
- Paolo B., Roberto B., Sebastian S., & Ruben S., T –  $\Omega$  Formulation for Eddy-Current Problems with Periodic Boundary Conditions, *IEEE Transactions on Magnetics*, 53 (2017).
- Emmanuel C., Serge N., & Roberta T., A guaranteed equilibrated error estimator for the A- $\phi$  and T- $\Omega$  magnetodynamic harmonic formulations of the Maxwell system, *IMA Journal of Numerical Analysis*, 37 (2017), 750 – 773.
- Chuan L., Ping Z., Dingsheng L., Bo H., & Dinkow S., Multiply Connected 3-D Transient Problem With Rigid Motion Associated With T- $\Omega$  Formulation, *IEEE Transactions on Magnetics*, 50 (2014).
- Gregor S., Iztok B., Miraleo H., Bojan Š., 2, Sebastijan S., Numerical modelling of linear generators, *PRZEGLĄD ELEKTROTECHNICZNY*, 95 (2019), 4-6.
- Minshuo C., Lei H., Peiwen T., Yang L., Ghulam A., & Minqiang H., A Stator-PM Transverse Flux Permanent Magnet Linear Generator for Direct Drive Wave Energy Converter, *IEE Access*, 9 (2021), 9949-9957.
- Mahesh P., Han-Sol K., Naveen K., Jong-Jin C., Woon-Ha Y., & Jongmoon J., Optimizing the design of wide magneto-mechano-electric generators to maximize their power output and lifetime in self-powered environmental monitoring systems, *nano Energy*, 114 (2023).
- Hongbo Q., Zhihao Z., Bin X., & Cunxiang Ya., Influence of Eddy Current Loss on Electromagnetic Field and Temperature Field of High-Speed Permanent Magnet Generator With the Toroidal Windings, *IEE Access*, 10 (2021), 98259-98267.
- Wenzhen L., Huihua F., Jian L., & Boru J., Electromagnetic-Thermal Characteristics Analysis of a Tubular Permanent Magnet Linear Generator for Free-Piston Engines, *Applied sciences*, 14 (2024), 1-16.
- Camayo K J., Quispe C., & Moggiano N., Electric Power Generation Modeling for an Experimental Biomimetic Turbine with Permanent Magnets in Places with Low Water Flow in the Mantaro Valley – Perú, *IOP Conference Series: Earth and Environmental science*, International Conference on Clean Energy and Electrical Systems, 812 (2021), 1-7.
- Armando M., Carlo B., Raffaele C., Raffaele S., & Pierpaolo N., Simulation methodology and numerical comparison of boxer and opposed free piston linear generator configuration in 0D/1D environment, *Applied Thermal Engineering*, 246 (2024).
- Cruz J., Ocean wave energy current status and future perspectives, *Green Energy and Technology*, 1 (2008), 1855 – 3537.
- Yong L., Zhang L., Lin z., Liu Q., Marine renewable energy in China current status and perspectives, *Water Science and Engineering*, 7, nr 3, (2014), 288-305.
- Daewoong S., Belissen V., Yeunga W., Performance validation and optimization of a dual coaxial-cylinder ocean-wave energy extractor, *Renewable Energy*, 92 (2016), 192 – 201.
- Besley PH., Wave overtopping of seawalls, design and assessment manual, *R&D technical report*, (1999), 1- 37.
- Hamel M., Mohellebi H., A LabVIEW-based real-time acquisition system for crack detection in conductive materials, *Mathematics and Computers in Simulation*, 167 (2020), 381 – 388.
- Kang T., Chen T., Wang Y., and Kim I., A t- formulation with the penalty function term for the 3d eddy current problem in laminated structures, *Applied Mathematics and Computation*, 271 (2015), 618-641.
- Bouillault F., Ren Z., and Razeq A., Calculation of 3d eddy current problems by an hybrid t-omega method, *IEEE Transactions on Magnetics*, 26 (1990), 478- 481.
- Man Kim J., Koo M., Jeong J., Hong K., Cho I., and Choi J., Design and analysis of tubular permanent magnet linear generator for small-scale wave energy converter, *AIP Advances*, 7, nr 5, (2017), 056630- 056635.
- Zaouia M., Benamrouche N., Djerdir A., Study and Analysis of an Electromagnetic Energy Recovery Damper (EERD) for Automotive Applications, *International Conference on Electrical Machines IEEE*, 12 (2012), 2716- 2721.